

Invited paper to be published in Memoirs of 556  
Kobe University, Japan in Oct. 1991.

Al<sub>x</sub>Ga<sub>1-x</sub>As SYNTHESIS BY KNOCK ON EFFECT OF ATOMS FROM Al  
FILMS ON GaAs BY As<sup>+</sup> IMPLANTATION

Rajpal S. DEOL\* and Toshihiko KOBAYASHI

Department of Electrical Engineering

Received on 9 October 1991

Abstract

The synthesis of Al<sub>x</sub>Ga<sub>1-x</sub>As by depositing thin films of Al on GaAs substrates and irradiating with arsenic ions has been studied using photoluminescence, transmission electron microscopy and secondary ion mass spectrometry. Following implantation secondary ion mass spectrometry has identified appreciable levels of Al to a depth of about 0.25 μm. AlGaAs emission within the photoluminescence spectra was seen for samples implanted with 1x10<sup>17</sup> cm<sup>-2</sup> of As<sup>+</sup> at 150 keV through an Al-film of thickness 580 Å and annealed at 950°C for 25sec. Transmission electron microscopy showed these layers to be single-crystal but characterised by dislocation loops of varying sizes.

1. Introduction

In the semiconductor industry ion implantation is an established technique for controlled dopant incorporation. Recently it has emerged as a powerful technique for material synthesis[1]. The material system Al<sub>x</sub>Ga<sub>1-x</sub>As/GaAs forms the basis of a number of commercially significant optoelectronic devices. There is considerable interest in the use of ion implantation for selective area AlGaAs synthesis to fabricate devices such as waveguides and light emitting diodes. The synthesis of AlGaAs by dual implants of As<sup>+</sup> and Al<sup>+</sup> into GaAs followed by rapid thermal

---

\*Present address: Optoelectronics Research Centre, University of Southampton, Southampton SO9 5NH, United Kingdom.

annealing (RTA) has previously been reported [2]. This paper reports a detailed study of the formation of AlGaAs by ion beam mixing of Al films on GaAs.

## 2. Experimental Details

Table 1 shows the implantation and processing details of the specimens generated using the ion beam mixing technique. Aluminium layers of 580Å or 650Å in thickness were deposited onto liquid encapsulated Czochralski (LEC) grown samples of semi-insulating <100> GaAs. The deposition was done using pure aluminium on a heated filament at a chamber pressure of  $\sim 10^{-6}$  Torr with the thickness being measured using a talystep. Subsequently As<sup>+</sup> implants were performed at room temperature using an energy of 150, 200 or 300 keV and a dose of  $3 \times 10^{16}$  or  $1 \times 10^{17}$  cm<sup>-2</sup>. The implantation energy was selected to ensure that the projected depth exceeded the thickness of the Al overlayer employed. Following implantation the residual Al layer was removed in 1 molar NaOH solution and the samples coated with a dual capping layer of  $\sim 400\text{\AA}$  Si<sub>3</sub>N<sub>4</sub> and  $\sim 600\text{\AA}$  AlN to inhibit surface decomposition during RTA using a double graphite strip heater. Following RTA the encapsulant was removed in HF and the layers assessed using photoluminescence (PL). The layers were studied before and after annealing using transmission electron microscopy (TEM) and prior to RTA using secondary ion mass spectrometry (SIMS). Experimental SIMS profiles showing the distribution of Al were compared with TRIM computer simulations.

Two millimetre square specimens were cleaved from the materials and prepared for plan-view TEM by mechanically polishing (from the back face) to a thickness of about 150μm prior to jet-chemical thinning with a 5% solution of bromine in methanol. During jet-etching Lacomit was used to protect the implanted surface. Conventional bright field (BF), centred-dark field (CDF) and selected area electron diffraction patterns (SADP) were recorded in a JEOL 200CX microscope operated at 200kV employing a double-tilt holder.

Dynamic SIMS analysis was performed using a Cameca IMS-3F machine employing a primary O<sub>2</sub><sup>+</sup> ion beam of energy 15keV and

positive secondary ion detection in order to optimise the sensitivity to Al. The beam was raster scanned over a  $250\mu\text{m}$  square area and the data collected from the central  $60\mu\text{m}$  square segment within this area. The relative sensitivity factor (RSF) for Al in GaAs was obtained from an implanted standard with a dose of  $1 \times 10^{17} \text{ Al}^+/\text{cm}^2$ . By measuring the sputtered crater depth using interference microscopy the depth scale was obtained within an accuracy of  $\pm 6\%$ .

Photoluminescence was excited from the specimens at 77K using the 514 and 488nm line of an  $\text{Ar}^+$  laser. The laser powers employed were 150mW and 10mW respectively. The emission was passed through a spectrometer and detected using a germanium p-i-n diode detector or GaAs detector with a R636 photomultiplier tube. The laser light was mechanically chopped and the detector output processed using standard lock-in detection.

Table 1 Specimen Details

Sample Number	Energy (keV)	Dose $\text{As}^+/\text{cm}^2$	Al layer thickness (Å)	Projected depth $R_p(\text{Å})$ for $\text{As}^+$ into Al
A	150	$3 \times 10^{16}$	580	830
B	150	$1 \times 10^{17}$	580	830
C	200	$1 \times 10^{17}$	650	1090
D	200	$3 \times 10^{16}$	650	1090
E	300	$3 \times 10^{16}$	650	1620

### 3. Results

Results pertaining to material B in which synthesis was achieved will be discussed below.

#### 3.1 SIMS

Figure 1 shows a SIMS profile of the distribution of Al in

material B following implantation and before RTA. The nature of the Al distribution is seen to be exponential in character with appreciable levels of Al to a depth of about  $0.25\mu\text{m}$ . Also shown in this figure is a theoretical atomic profile for Al determined using TRIM [3] (Transport of Ions in Matter). This computer simulation package relies on LSS [4] (Lindhard, Scharff, Schiøtt) range statistics and predicts the interstitial distribution. The theoretical interstitial distribution of Al is seen to agree well with the SIMS profile.

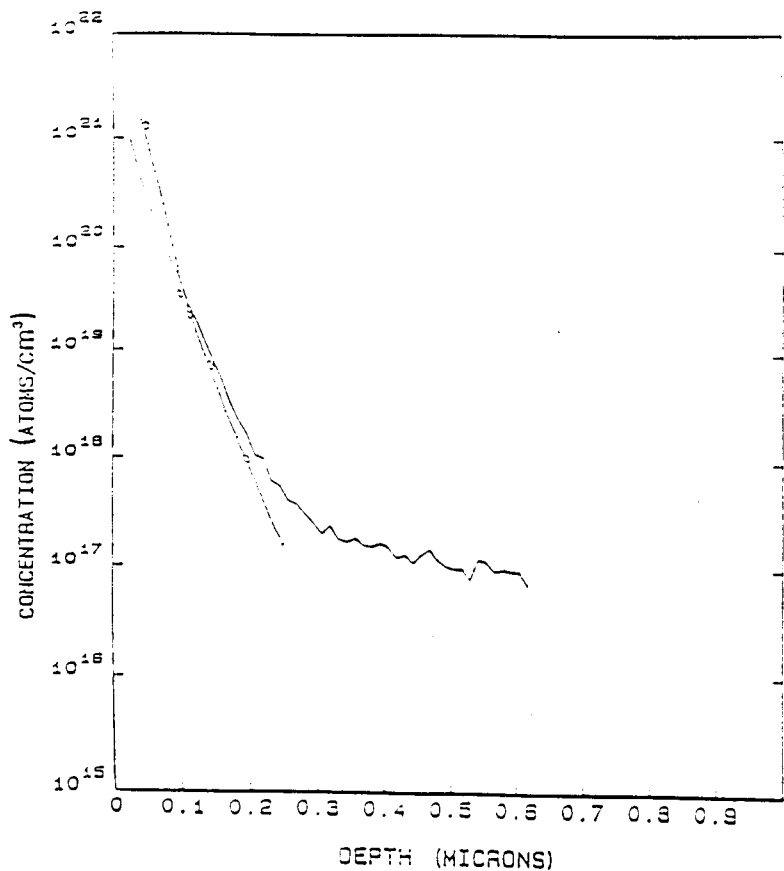


Fig.1. TRIM (---) data and SIMS profile of Al (-) in material B prior to RTA.

### 3.2 PL

Figure 2(a) shows a PL spectra obtained at a temperature of 77K from material B following RTA using an excitation wavelength of 514nm and a germanium p-i-n diode detector. A broad emission extending from above the GaAs band edge to shorter wavelengths is seen which we attribute to the formation of  $\text{Al}_x\text{Ga}_{1-x}\text{As}$  of varying  $x$ . The majority of the emission occurs at about 780nm

corresponding to an AlGaAs composition of  $x=0.06$  [5]. Figure 2(b) depicts a PL spectra obtained from the same material at a temperature of 77K but using an excitation wavelength of 488nm and a GaAs detector with a R636 photomultiplier tube. This detector is more sensitive in the wavelength range 900 to 300nm. A broad emission from about 900nm to shorter wavelengths is seen which we attribute to  $\text{Al}_x\text{Ga}_{1-x}\text{As}$  formation of varying  $x$ . The majority of the emission occurs at 640nm corresponding to an  $\text{Al}_x\text{Ga}_{1-x}\text{As}$  composition of  $x=0.334$  [5].

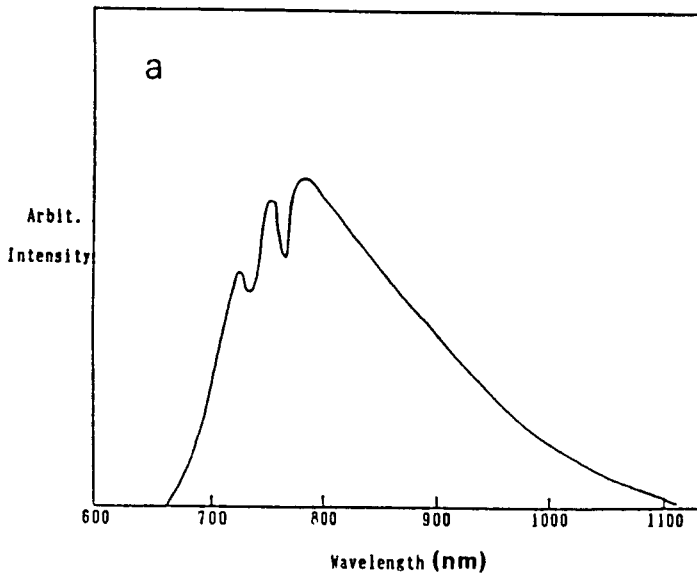
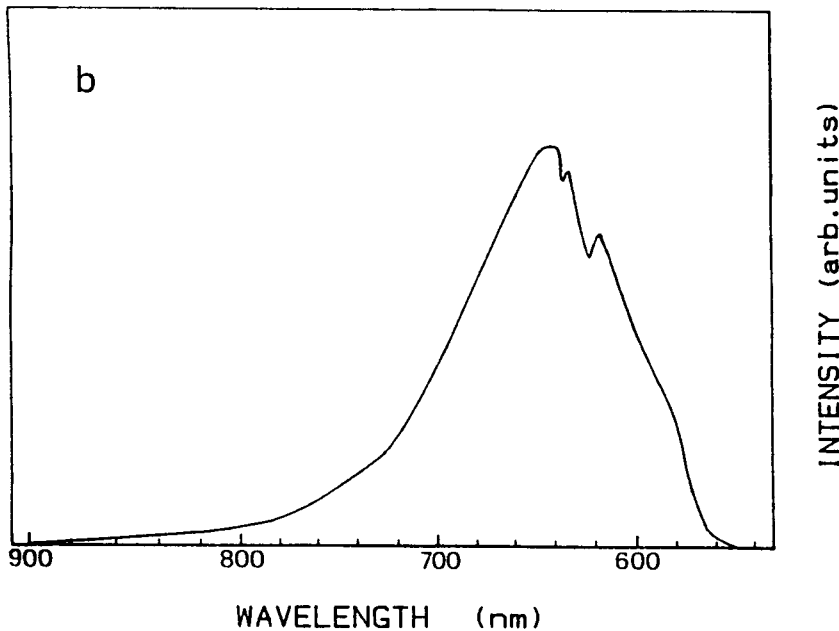


Fig.2. PL spectrum obtained at a temperature of 77K from material B.



The differences between the two PL spectra relate to

differences in detector efficiency over the wavelength domain of interest and the difference in the excitation wavelength. Namely the PL spectra in Figure 2(b) was obtained using a shorter excitation wavelength than Figure 2(a) and so the sampling depth was nearer to the specimen surface where the AlGaAs composition contains a higher concentration of Al.

### 3.3 TEM

TEM in a plan-view configuration was used to study the microstructure of material B in the as-implanted state and as function of annealing temperature. Figure 3(a) is a BF image obtained from material B prior to RTA. Apparent are a high density of interstitial point defects which, in view of the SIMS and TRIM data, are likely to be Al in composition. The selected area electron diffraction pattern associated with this material prior to RTA is shown in Figure 3(b). The diffraction pattern has been taken with a 001 beam direction. There is streaking and splitting of the reciprocal lattice points in the  $\langle 110 \rangle$  directions. This is indicative of the lattice being highly strained.

Figure 4 illustrates the defect structure associated with material B following RTA. The synthesised AlGaAs layer is characterised by dislocation loops of varying sizes. The loop sizes fall into three categories less than or approximately equal to 20nm, between 30 to 50nm and ~90nm with loops of diameter

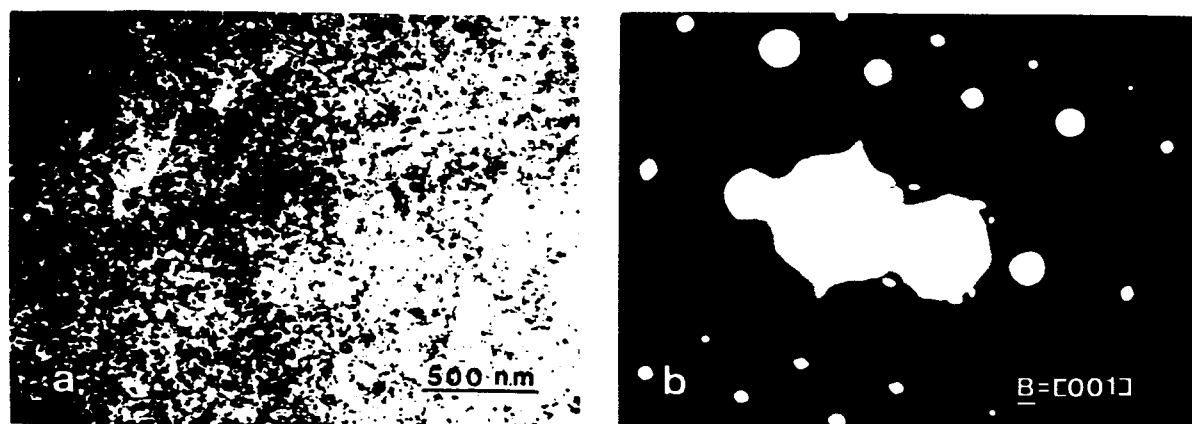


Fig.3. (a) BF image and (b) electron diffraction pattern from material B before RTA.

~90nm being least in number. It is likely that the majority of the dislocation loops are of interstitial character and of  $1/2\langle 110 \rangle$  type. The electron diffraction patterns associated with this layer were single crystal spot patterns without any distortions of the reciprocal lattice points.

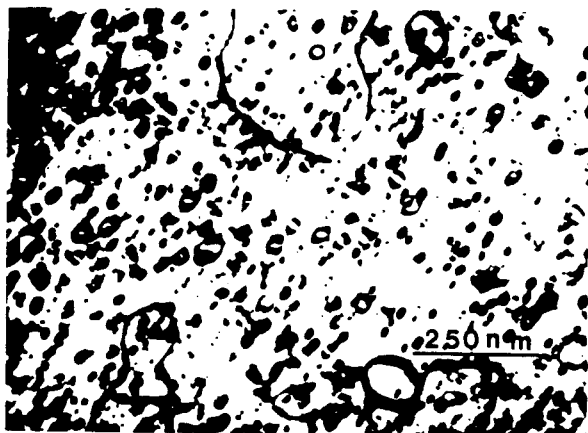


Fig.4. BF image of material B following RTA.

#### 4. Conclusions

The nature of the Al distribution, revealed by SIMS, in the GaAs matrix following implantation has been correlated with TRIM simulations showing interstitial distribution.

Synthesis of  $\text{Al}_x\text{Ga}_{1-x}\text{As}$  has been achieved for  $\langle 100 \rangle$  GaAs substrates implanted with  $1 \times 10^{17} \text{ cm}^{-2}$  of  $\text{As}^+$  at 150 keV through an Al-film of thickness 580Å and annealed at 950°C for 25 seconds. The composition of the AlGaAs layer has been shown to vary with depth from the specimen surface.

The synthesised AlGaAs layer contains dislocation loops of varying sizes and the associated electron diffraction patterns are single crystal spot patterns without any distortions of the reciprocal lattice points. Prior to RTA the implanted GaAs substrates were characterised by point defects which were inferred to be Al in composition and the level of strain was sufficient to distort the reciprocal lattice points.

## 5. Acknowledgements

One of the authors (RSD) wishes to thank the Royal Society and the Japan Society for the Promotion of Science for financial support.

## 6. References

- [1] Jeynes, C.: Novel Applications of Ion Implantation, Vacuum 39, 1047-1056, (1989).
- [2] Deol, R.S. et al.: Synthesis of AlGaAs by  $\text{As}^+$  and  $\text{Al}^+$  Implants into GaAs, Inst. Phys. Conf. Ser., 100, 127-132, (1989)
- [3] Biersack, J.P. and L.G. Haggmark: A Monte Carlo Computer Program for the Transport of Energetic Ions in Amorphous Targets, Nucl. Instrum. Methods, 174, 257-269, (1980)
- [4] Lindhard, J., M. Scharff and H.E. Schiøtt: Kgl. Danske Videnskab., Mat. Fys. Medd. 14, 33, (1963)
- [5] Adachi, S.: GaAs, AlAs and  $\text{Al}_x\text{Ga}_{1-x}\text{As}$ : Material Parameters for use in Research and Device Applications, J. Appl. Phys. 58, R1-R29, (1985)